45th CANADIAN GEOTECHNICAL CONFERENCE
45e CONFERENCE CANADIENNE DE GEOTECHNIQUE

PREPRINT VOLUME

INNOVATION CONSERVATION and RENOVATION

October 26 to 28, 1992

The Royal York Hotel
Toronto, Ontario

SPONSORED BY

THE CANADIAN GEOTECHNICAL SOCIETY

LA SOCIÉTÉ CANADIENNE DE GÉOTECHNIQUE

Printed on Recycled Paper

ISBN 0-920505-

Prediction of Moisture Movement in Highway Subgrade Soils

S. Lee Barbour, Delwyn G. Fredlund, Julian K-M Gan, G. Ward Wilson
University of Saskatchewan, Saskatoon, SK

ABSTRACT

The performance of a highway is strongly influenced by the moisture conditions in the subgrade. The predictions of the moisture movement in the subgrade soil requires formulations for flow in the saturated and the unsaturated porous media, as well as for flow due to thermal gradients. Flow due to thermal gradients will not be covered in this paper. Modelling of moisture movement using the formulations just described are presented for a typical highway structure. Matric suction is an independent stress state variable which affects the total head for flow, and the hydraulic conductivity of the unsaturated medium. Special devices are required for the measurement of matric suction in the field. Two case histories involving thermal conductivity sensors for matric suction measurements in the field are described.

INTRODUCTION

Highway engineering has, to a large extent, remained at the periphery of geotechnical engineering. Many aspects associated with highway design began on an empirical basis and required years of practical experience to establish their credibility. Probably the most classic example of this approach to design is the use of the California Bearing Ratio test which produces a CBR value. The California Bearing Ratio test has been in use since 1929, a period of more than 60 years (Tschebotarioff, 1951) and still forms the basis for most highway pavement structural designs. All this is not too surprising since much of pavement design preceded the development of modern soil mechanics.

Theoretical and technological developments in modern soil mechanics have given primary attention to saturated soils under positive pore-water pressures. At the same time, many of the engineered works of man, such as roads, have involved the compaction of unsaturated soils. These soils are compacted at a degree of saturation of approximately 80 to 85 percent and have negative pore-water pressures which may range from one atmosphere or less for silty soils to many atmospheres for clayey soils. The negative pore-water pressure provides the soil with high interparticle stresses and as a result, substantial shearing resistance.

Only during the past decade or so has a theory and technology emerged for unsaturated soils which is applicable to compacted materials. Theoretical analyses utilizing unsaturated soil mechanics theory have been proposed for all the classic soil mechanics problems; namely volume change and deformation, shear strength and stability, and fluid flow. All three of these categories are of interest in the design of pavement structures.

The initial design of a pavement structure (i.e., surface, sub-base, base and subgrade) can be viewed as a bearing capacity problem involving the shear strength of the compacted unsaturated soils (Broms, 1965). At the time of construction, the shear strength of the subgrade is high due to the negative pore-water pressures. As such, the highway has a high bearing capacity and functions as designed. With time, however, there is an ingress of water into the weakest part of the pavement structure (i.e., the subgrade). The result is an increase of the roughness index of the pavement surface due to volume change and distortion of the subgrade soils. This is followed by a reduction in the bearing capacity of the pavement. This suggested model of pavement behavior may be somewhat simplistic, however, it identifies the primary mechanisms involved.

This paper considers the behavior of flexible pavement roadways. A flexible pavement would remain essentially as built, were it not for the ingress of water through the base and subbase courses, into the subgrade. This description assumes that overloading of the pavement structure does not occur and as a result, pavement fatigue cracking is not a primary factor. Consequently, it appears reasonable that the factors controlling the movement of water into the pavement structure system should be of primary interest to the prediction of changes in the condition of the highway. Considering recent developments in the area of saturated-unsaturated flow modelling, the question that is addressed is, "What new lessons can be learned concerning pavement design from saturated-unsaturated flow modelling?"

The modelling of water movement in the substructure of a pavement requires a quantification of the surface flux boundary conditions. Water may leave the surface of the shoulder and ditch of the roadway through the processes of evaporation (or evapotranspiration). On the other hand, water may enter the roadway as a result of rainfall or snowmelt. In other words, the surface boundary is controlled by the microclimate at the site as shown in Figure 1.

Numerous attempts have been made in recent years to measure negative pore-water pressures in highway subgrade soils. These attempts have been met with mixed success. The primary objective of saturated-unsaturated flow modelling is to be able to predict changes in negative pore-water pressure in subgrade soils as a result of changes of the microclimate environment. Computer modelling needs to be confirmed with insitu measurements in order to establish confidence in the procedure. However, parametric type numerical modelling studies can play a valuable role in

quantifying the relative importance of various design considerations.

FLOW THROUGH UNSATURATED SOILS

The physics of flow through saturated soils is well established. At the same time, it is recognized that the primary soil property required for analytical purposes, i.e. coefficient of permeability, is highly variable and it is difficult to obtain a representative value of insitu conditions. When giving consideration to unsaturated soils, the problem becomes even more difficult since the coefficient of permeability is a function of the negative pore-water pressure (or the water content) of the soil.

The flow of liquid water in an unsaturated soil also occurs in accordance with Darcy's law. This means that flow takes place in response to a hydraulic head gradient where the coefficient of permeability gradient is a function of the negative pore-water pressure.

$$v = -k_w(u_w)\frac{\partial h}{\partial y} \qquad [1]$$

where v = Darcy velocity or unit discharge (L/T)

y = cartesian coordinate direction (L)

h = hydraulic head (L) consisting of an elevation head, y, and pressure head $u_w/(\rho_w g)$ (i.e., $h = y + \frac{u_w}{\rho_w g}$), where ρ_w = density of pore fluid, g = acceleration due to gravity

$k_w(u_w)$ = hydraulic conductivity with respect to the water phase as a function of the pore water pressure (u_w). (L/T)

The partial differential equation of transient flow through a homogeneous, anisotropic unsaturated soil can be written by applying Darcy's law, while satisfying the conservation of mass of the water phase.

$$\frac{\partial}{\partial x}\left(k_x(u_w)\frac{\partial h}{\partial x}\right) + \frac{\partial}{\partial y}\left(k_y(u_w)\frac{\partial h}{\partial y}\right) = m^w_2\frac{\partial u_w}{\partial t} \qquad [2]$$

where t = time

x,y = cartesian coordinate directions

m^w_2 = volumetric modulus representing a change in volume of water with respect to a change in matric suction, $(u_a - u_w)$.

Equation 2 has the same form as for a saturated soil except that the permeability is now a function of pore-water pressure, which in turn, is a function of hydraulic head. As a result, the equation is nonlinear.

It is the pore-water pressure which is the primary variable of interest from the solution of the seepage equation. This is in contrast to other types of seepage problems where the interest may lie in attempting to compute quantities of flow. The computed pore-water pressures are quite insensitive to the permeability and the permeability function used in the analysis when only one soil type is present (Papagianiakis and Fredlund, 1984). This is in contrast to the computation of the quantity of seepage which is highly dependent upon the coefficient of permeability. In a layered system of soils, however, the interaction of flow from one soil layer to another can influence the computed pore-water pressures.

The relationship between the volumetric water constent and the negative porewater pressure defines the ability of the soil to retain water under increasing suction and is often referred to as the moisture retention curve. The slope of this curve, m^w_2, represents the modulus of volume change for the fluid phase with respect to changes in matric suction (Fredlund and Morgenstern, 1976). The moisture retention curve is also significant because it is often used as the basis for estimating the relationship between hydraulic conductivity and matric suction, to be discussed later in this section.

The measurement of the relationship between volumetric water content can be performed with the aid of a pressure plate device often referred to commercially as a 'Tempe'[1] cell. The device consists of a cell in which a high air entry disk (HAED) has been sealed into the base. A saturated soil sample is placed on a saturated HAED which is connected to a free draining reservoir. The cell is then sealed and connected to an air pressure line. Increases in suction $(u_a - u_w)$ can be obtained by increasing the air pressure, u_a, while keeping the water pressure in the sample at atmospheric conditions. The sample is allowed to come to equilibrium under a series of increments in air pressure. Measurement of the amount of water drained from the sample under each increment of air pressure allows the volumetric water content of the sample at each load of suction to be calculated.

The relationship between the coefficient of permeability and suction for an unsaturated soil is difficult to measure. For geotechnical engineering purposes, the permeability function is often computed from the moisture characteristic curve for the soil (Mualem, 1986). Starting from the saturated coefficient of permeability, the permeability corresponding to various matrix suctions is computed. This is based on the assumption that the volumetric water content at a particular value of suction represents both the cross sectional area available for flow and the effective diameter of the fluid filled pores (Childs and Collis-George (1950), Millington and Quirk (1961), Green and Corey, (1971)). These empirical functions can be computed in accordance with the procedure described by Brooks and Corey, (1964) and Green and Corey, (1971). It is also possible to best-fit the permeability versus matric suction relationship with a closed form mathematical function such as that proposed by Gardner (1958), Van Genuchten (1980) and others.

Once the permeability function of the soils involved are known, the pore-water pressures can be computed by solving Equation 2 using an iterative procedure (Lam et al. 1982).

PHYSICS OF THE FLUX BOUNDARY CONDITION

The surface of a section transverse to a highway (Fig. 1) shows that part of the roadway is covered by an impermeable layer (i.e., asphalt). It should be made clear that while the asphalt surface is an initially continuous layer, it deteriorates with time and cracking progressively occurs. However, for the purposes of this paper, it is assumed to be impervious, and therefore prevents infiltration and evaporation (i.e. zeroflux). The shoulder of the roadway may or may not be covered with asphalt and the ditch portion is generally grassed. The unpaved shoulder and grassed sections are subjected to a flux boundary condition related to the climate in the immediate vicinity.

[1] Tempe is a brand name of Soil Moisture Corporation, Santa Barbara, California.

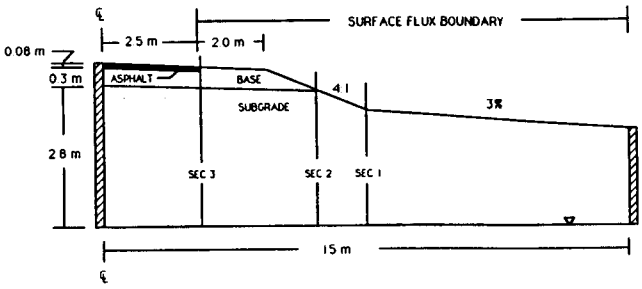

Figure 1 Typical cross-section through a highway showing the surface boundary controlled by microclimatic conditions.

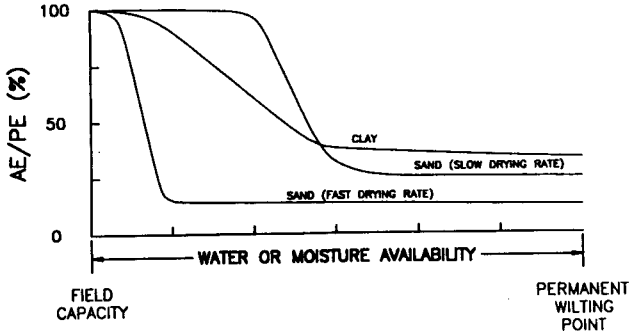

Figure 2 The ratio of the actual rate of evaporation and potential evaporation, AE/PE, versus water availability (after Holmes, 1961, and Gray, 1970).

Rainfall on the pavement runs off and infiltrates into the shoulder of the highway. Rainfall on the remainder of the shoulder and ditch may seep into the ground and in some cases there may be significant runoff. The quantification of precipitation (and snowmelt) can be obtained directly from microclimatic data.

The upward, evaporative flux of water from the roadway is difficult to quantify. Most analytical tools available to-date, provide an estimate of the potential rate of evaporation from an open water or saturated surface. The rate of potential evaporation from a saturated surface is an upper limit or maximum rate of evaporation determined on the basis of climatic conditions (i.e. temperature, relative humidity, solar radiation and wind speed). In general, the rate of evaporation from the shoulder and ditch area of the pavement structure is equal to the potential rate of evaporation when the surfaces are wet or saturated. This high rate of evaporation continues only as long as the surface remains at or near saturation. The actual rate of evaporation declines significantly when the soil surfaces become unsaturated.

Figure 2 after Holmes (1961) and Gray (1970) shows the ratio of actual evaporation 'AE', and potential evaporation 'PE' versus soil suction at the ground surface for clay and sand surfaces. It can be seen that both the clay and sand surfaces evaporate at a potential rate (i.e. AE/PE equal 100 %) when the value of soil suction is low. However, the actual evaporation rate from a sand surface which has been allowed to dry for an extended period may be only 5 to 10 percent of the initial potential rate of evaporation. Clay on the other hand can maintain a near potential rate of evaporation for an extended period of time compared to sand. This phenomena is significant as the texture of the soils forming the shoulder, embankment and ditch greatly effect the evaporative fluxes which occur between rainfall events.

In addition to soil texture, the groundwater regime also influences evaporative fluxes. For example, the actual rate of evaporation will remain equal to the potential rate of evaporation if the groundwater table is at or very near the ground surface. Wilson (1990) showed that maintaining the water table within 0.5 meters of the ground surface in a fine sand allows the rate of evaporation to continue at the full potential rate for an extended period of time. Alternately, lowering the water table to 1.0 meter below the surface of the sand causes the actual rate of evaporation to decrease to 10 percent of the initial potential rate of evaporation after 2 days of drying.

The method of predicting actual evaporative fluxes is complex and is not described here. Wilson (1990) provides a method of evaluating evaporative fluxes from soil surfaces. The method uses a modified Penman method to calculate actual soil evaporative fluxes on the basis of soil suction and temperature at the ground surface. The values of suction and temperature at the soil surface are determined by solving a coupled system of equations for heat and mass transfer below the soil surface.

In summary, the texture of a soil surface and position of the groundwater table affect the flux boundary conditions with respect to water flow at the ground surface. Sand and gravel surfaces have a high infiltration rate compared to silty and clayey soil surfaces. In contrast, clayey and silty soil surfaces maintain a higher rate of evaporation than granular soils during dry periods. The combined effect of these infiltrative and evaporative features are strongly coupled with the groundwater regime. In general, the net flux boundary condition (i.e. total precipitation less runoff and evaporation) at the soil surface is higher for granular surfaces and lower for clay surfaces under identical climatic conditions. In some cases, the net flux boundary condition for a granular surface can exceed that for a clay surface by as much as a factor of 10 given the same climatic conditions.

Factors such as those described above have a significant effect on the moisture regime within the subgrade and embankment below the pavement structure. For example, consider the performance of a road structure with a clay subgrade and clean granular shoulder. High infiltration and low evaporation rates will occur across the surface of the shoulder. The subgrade below the shoulder and pavement will tend to a wet condition with a high water table. The values of suction will decline and a loss in bearing capacity will occur. Increasing the clay and silt content of the granular shoulder surface will reduce infiltration and increase evaporation rates. This will have the net effect of reducing the flow of water into the subgrade clay and hence prevent the loss of strength.

MODELLING OF MOISTURE MOVEMENT IN PAVEMENT STRUCTURES

A simplified pavement cross-section will be used in order to illustrate the role that surface fluxes and saturated/unsaturated flow has on moisture movement within pavement structures. This typical section is based on a Saskatchewan Department of Highways standard cross-section and consists of 80 mm of asphaltic concrete over 300 mm of base (Figure 1). It is assumed that the subgrade consists of a silty clay. The volumetric water content and hydraulic conductivity versus suction relationships for the two soils in the section are shown in Figures 3a and 3b. The saturated hydraulic conductivity of the base is approximately 2 orders of magnitude greater than that of the subgrade. The asphaltic concrete is assumed to be impermeable.

The saturated/unsaturated flow model, SEEP/W (GEO-SLOPE, 1991) was used for all simulations. The finite element grid for the simulations is shown in Figure 4. Both steady state and

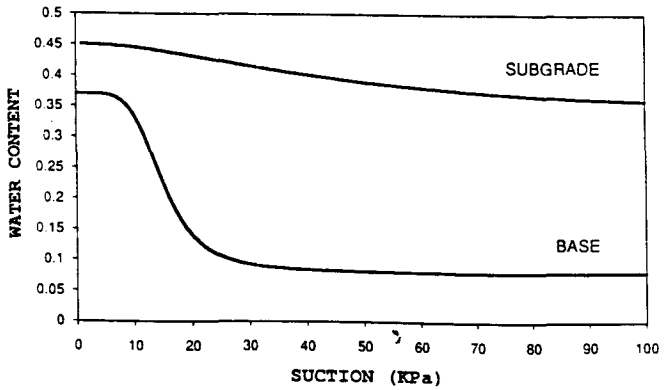

Figure 3a Volumetric water content versus suction relationships.

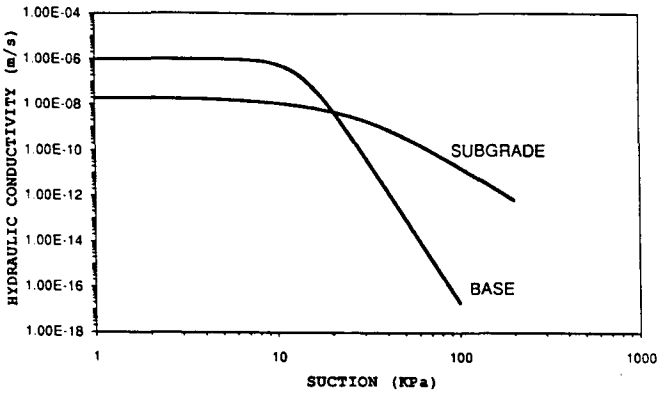

Figure 3b Hydraulic conductivity versus suction relationships

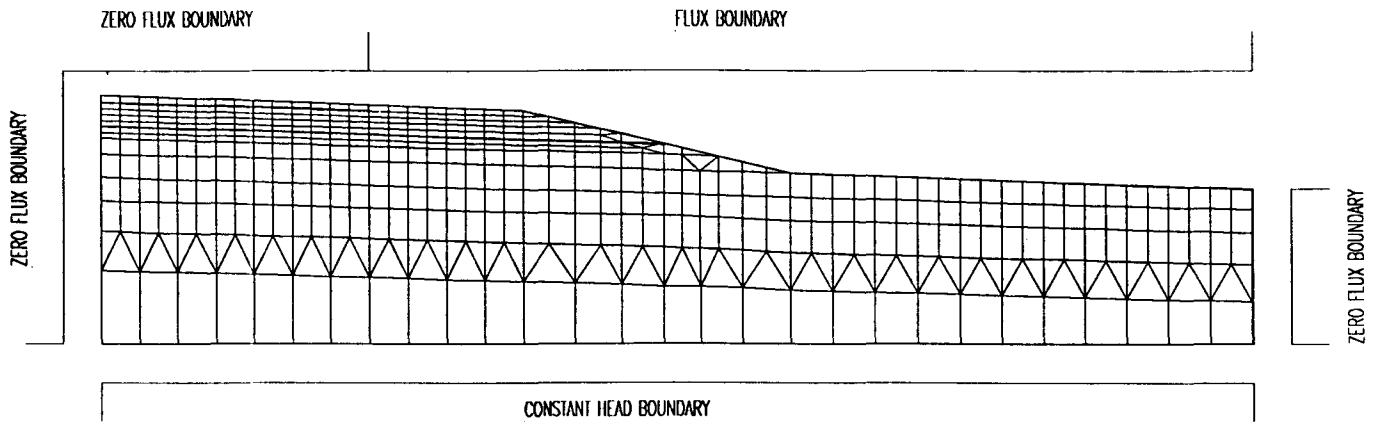

Figure 4 Finite element grid of highway cross-section.

transient simulations of moisture movement through the subgrade were conducted. The boundary conditions consist of zero flux along the left and right side of the section, a constant head boundary, representing a water table condition along the base of the section, and flux boundaries applied over the soil surfaces. Infiltrative and evaporative fluxes were used for the various cases.

The simulation cases are outlined in Table 1. Three steady state infiltration cases were run using applied flux rates equal to 1/10, 1, 10 times the saturated hydraulic conductivity of the subgrade. If the model is unable to accept all of this flux without ponding, it adjusts the surface to a zero pressure condition (i.e. flux that cannot be accepted is allowed to runoff).

A single steady state evaporation case was run with the distribution of evaporations outlined in Table 1. The distribution of evaporative fluxes across the section represent the maximum long-term, steady-state fluxes that can be applied to the surface of the section without the suctions at the surface exceeding 3000 kPa. Wilson (1990) demonstrated that at this magnitude of suction, the actual evaporation from a soil surface begins to be suppressed. A limit of 1500 kPa suction (i.e. the wilting point) is often used as the limiting suction that can be developed before evapotranspiration from plants begins to decline.

A simple one dimensional calculation of this limiting condition can be done on a spreadsheet using the method proposed by Kisch (1959) and described by Barbour (1990). Figure 5a, 5b, 5c illustrated the pressure profile across Sections 1, 2 and 3 (Figure 1), under the maximum evaporation rate for each section. It is apparent that because of its higher elevation and lower air entry value, the evaporation that can be sustained through the sand base is only a fraction of that produced through the subgrade, particularly in the ditch, where the subgrade overlies a shallow water table. The "break" in the pressure profile in Figure 5a, 5b and 5c represents the zone in which the suctions exceed the air entry value of the material and the coefficient of permeability begins to decline rapidly.

Transient simulations were also made of the redistribution during evaporation following steady-state infiltration. The initial pressure conditions in the section were taken as those developed under a steady-state infiltration of 1.7 mm/day. The evaporation rate was set at a potential evaporation of 2 mm/day.

The pressure distribution and moisture movement within the pavement structure during steady state infiltration is illustrated in Figures 6, 7 and 8. It is evident that under a low infiltration rate of .17 mm/day, predominantly vertical flow of water down to the water table takes place across the section. Although lateral flow of water under the pavement does occur through the base and subgrade, the suction at the top of the subgrade remains at approximately 25 kPa. Under the applied flux of 1.7 mm/day strong lateral flows in the base and subgrade occur, even though positive pressures and saturated conditions conditions do not develop. The suctions in the subgrade under the center of the roadway are still greater that 10 kPa. Under the large steady state fluxes of 17 mm/day a large portion of the base and subgrade below the shoulder becomes saturated. Strong lateral flows right to the center of the pavement structure are evident and the suctions under the center of the pavement drop to 2 kPa.

TABLE 1-- Applied Fluxes for Model Simulation

Case:	Surface Location	Applied Flux:
1. Steady State Infiltration - q = .1 Ks (subgrade) - q = 1 Ks (subgrade) - q = 10 Ks (subgrade)	- all soil surfaces	$+2x10^{-9}$ m/s (.17 mm/day) $+2x10^{-8}$ m/s (1.7 mm/day) $+2x10^{-7}$ m/s (17 mm/day)
2. Steady State Evaporation	- base sand (shoulder) - subgrade (mid-slope) - subgrade (ditch)	- .006 mm/day - .15 mm/day - .26 mm/day
3. Transient Case - Evaporation after Steady State Infiltration		
- Initial Condition based on Steady-State Infiltration Rate	- all soil surfaces	- $2x10^{-8}$ m/s (1.7 mm/d)
- Evaporation Rate	- all soil surfaces	- 2.3×10^{-8} m/s (2mm/d)

These flows and pressure distributions are in strong contrast to those developed under evaporative conditions (Fig. 9). Under evaporative conditions, there is strong flow up through the subgrade across the ditch and backslope. However, little flow occurs near the center of the pavement structure. In fact, below the center of the pavement structure, the pressure distribution is hydrostatic. The steady state cases illustrate that whereas infiltration events provide a mechanism by which moisture can be redistributed under the pavement structure, evaporative conditions are only effective in removing moisture from the subgrade along the shoulder and ditch.

The changes in the suction within the subgrade with time for the transient case are illustrated in Figures 10a, 10b and 10c. It is interesting to note that even after 10 days of evaporation the low suctions developed below the pavement structure under infiltration (Figure 7) have not been removed. Aitchison and Richards (1965) presented similar findings from an extensive field study of moisture conditions in pavements subgrades throughout Australia. Measurements from 15 instrumented sites of various subgrade materials and subsoil conditions show that the subgrade below a pavement structure reaches an equilibrium water content and varies little over time. The moisture condition of the subgrade beyond the pavement structure, however, show appreciable seasonal variations. Figure 11 from an instrumented site near Horsham in the state of Victoria, Australia, is typical of the data obtained. The matric suctions at the Horsham Site recorded at different seasons for the year 1958 are presented in Figure 12.

These simulations are obviously limited. They do not take into account cracks in the concrete, non-isothermal moisture movement, and other complications. They do, however, illustrate several crucial points. First, the dominant mechanism for moisture movements into the pavement structure is saturated/unsaturated flow as driven by the surface fluxes at the soil/atmosphere surface. Second, because of the geometry of the section and the contrast in both the saturated and unsaturated hydraulic properties (hydraulic conductivity and volumetric moisture content relationships) of the base and subgrade, there will always be a preferential wetting of the subgrade over time. Obviously, alternative design strategies for minimizing infiltration could be employed. These may include features such as extending the asphalt concrete over the shoulder or placing lateral drains along the edge of the pavement structure. For example, Figure 13 illustrates the pressure distribution under an infiltration rate of 1.7 mm/day when the asphalt is extended to the shoulder. It is evident in comparing this figure with Figure 7 that extending the asphalt doubles the suction under the center of the roadway. It is evident that the final performance of the roadway will depend on the long-term moisture redistribution within the pavement structure as controlled by surface fluxes and saturated/unsaturated flow.

FIELD MEASUREMENTS OF MATRIC SUCTION

Field application of some of the preceding theoretical concepts requires that means be available for the measurement of matric suction. The difficulty in the measurement of matric suction has been a major obstacle in the advancement of the mechanics of unsaturated soil media. The direct measurement of matric suction in the field is difficult. At the present time, matric suctions in excess of 1 bar cannot be measured directly in the field. Various indirect measurement techniques for matric suction greater than 1 bar have been developed. The reliability of most of these indirect techniques, however, is poor. In recent years, an indirect technique based on the relationship of the matric suction and the thermal conductivity of a reference porous ceramic has been developed. These so called thermal conductivity matric suction sensors have been used in the laboratory and in the field for some years now. The technique appears promising in terms of its principle of operation.

A thermal conductivity sensor which uses an integrated circuit as its heat sensing element is shown in Figure 14. The sensor consists of a porous ceramic block containing a temperature sensing device and a miniature heater. The water content of the ceramic is controlled by the water content versus matric suction relationship of the porous ceramic. An ideal ceramic is one with a wide range of pore size distributions. The rate of heat dissipation within the block is directly proportional to the water content of the block. The undissipated heat which causes a temperature rise is then inversely proportional to the water content in the block. The temperature rise can be calibrated to measure matric suction in the soil.

The thermal conductivity method of matric suction measurement is amenable to use in remote areas and automatic data acquisition systems. This enhances the versatility of the method.

One notable case of matric suction measurement conducted recently involves the instrumentation of matric suction beneath a full-scale pavement structure in the indoor circular test track facility of the Saskatchewan Department of Highways and Transportation in Regina, Saskatchewan. The cross sections of the track and the locations of the sensors are shown in Figure 15.

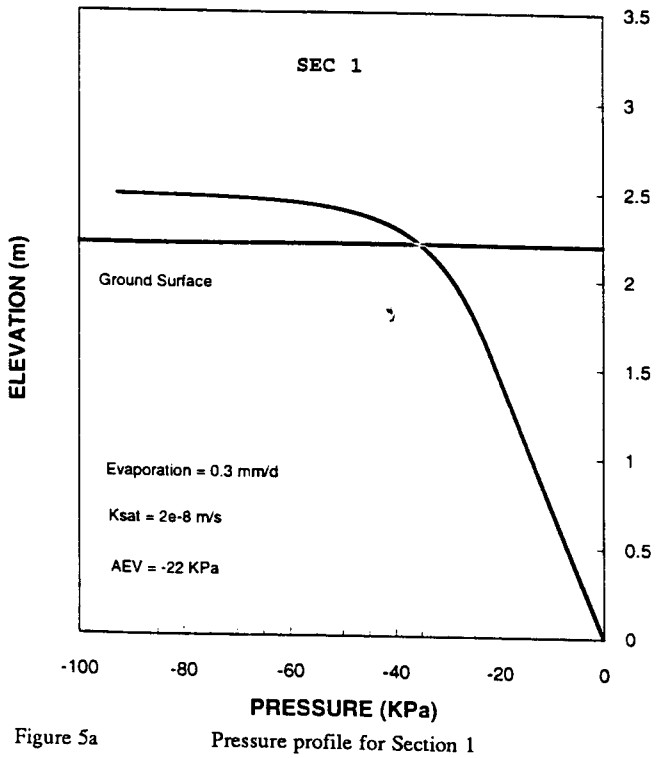

Figure 5a Pressure profile for Section 1

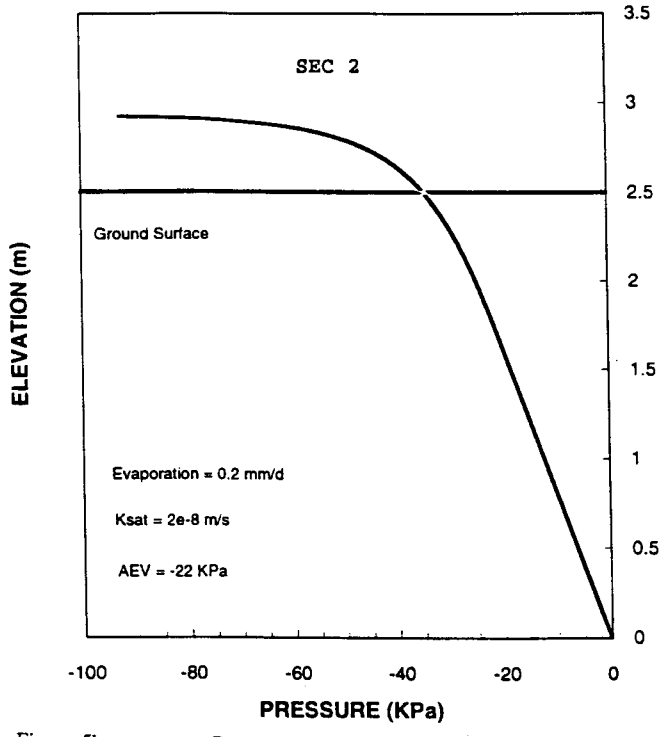

Figure 5b Pressure profile for Section 2

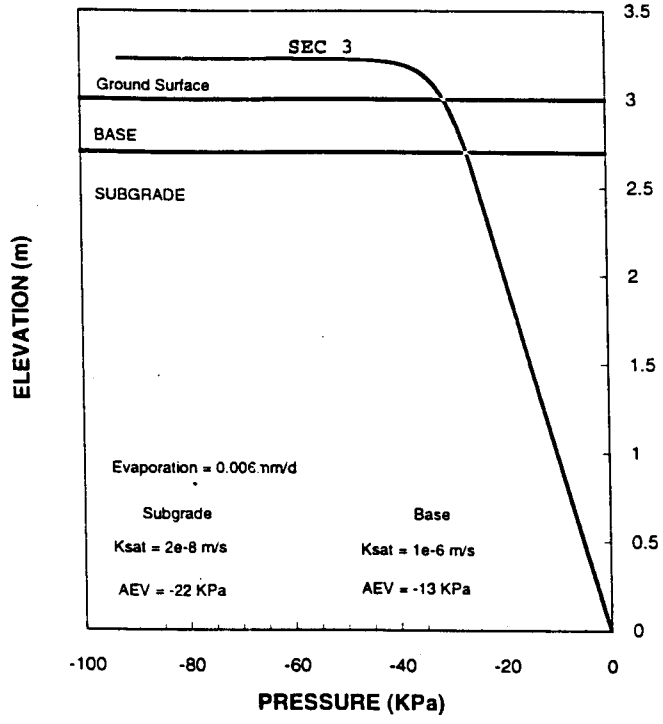

Figure 5c Pressure profile for Section 3

Most of the sensors were installed in dry vertical drill holes. However, for some of the sensors in the deep holes, water was added. This unfortunate procedure was adopted at the discretion of the engineer on site in order to facilitate the installation procedure which was difficult at those depths. The matric suction values recorded by these sensors were observed to decrease rapidly to values of less than 30 kPa, and remained low over the entire monitoring period (Figure 16). The pre-wetting of the hole was an unfortunate innovation to the installation procedure as the added water appeared to be slow to redistribute throughout the soils.

Long term, stable measurements were obtained from the thermal conductivity sensors. Some typical data obtained over a monitoring period of one year are presented in Figures 17 and 18. These results show that the glacial till and the Regina clay placed at near optimum water content conditions has equilibrium matric suction values of about 50 kPa in the glacial till, and 400 kPa to 500 kPa in the clay, respectively.

The responses of the thermal conductivity sensors during the infiltration test where the sideslopes were inundated, are presented in Figure 19 and Figure 20. The responses of these sensors showed that the water travelled to the sensor locations in the clay subgrade in a matter of a few hours to a day after flooding. The matric suciton values decreased to zero rapidly (less than 1 hour, in some cases). The high flow of water is suggestive of an extensive network of secondary desiccation cracks in the clay. Extensive cracks will lead water into the sand layer at the base, conveying water rapidly to the interior section of the subgrade. The responses of the sensors in the till subgrade were more varied and some sensors showed a considerably slower and more gradual infiltration of water to the sensor locations (Figure 20).

Observations made during the excavation to retrieve the sensors at the end of the program showed that there were preferential flows along the wires leading to the sensors. This was likely due to a poor backfilling procedure for the sensors. This problem is probably augmented by the vertical orientation of the installation boreholes. More recent techniques of installation are carried out in trenches or caisson holes, with the sensors installed at an upward slope into the side walls.

Matric suction values of less than zero were recorded for some of the sensors after ponding. Thermal conductivity sensors measure matric suction indirectly by correlating the temperature rise due to a controlled heat pulse being applied for one minute. In

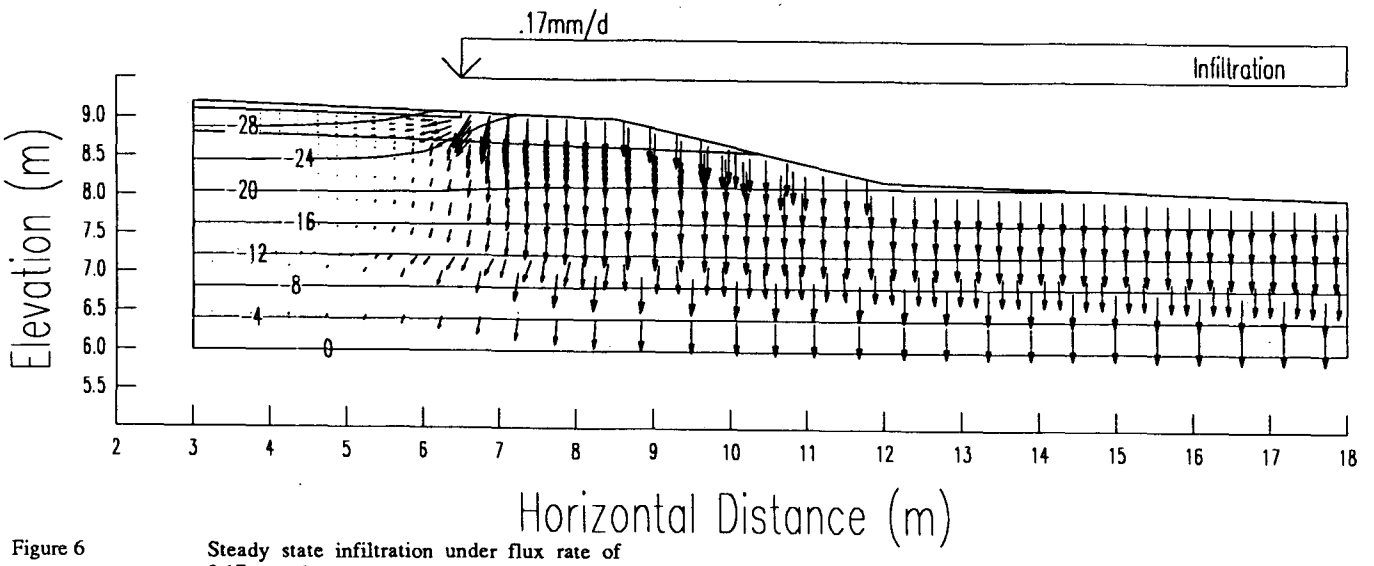

Figure 6 Steady state infiltration under flux rate of 0.17 mm/d.

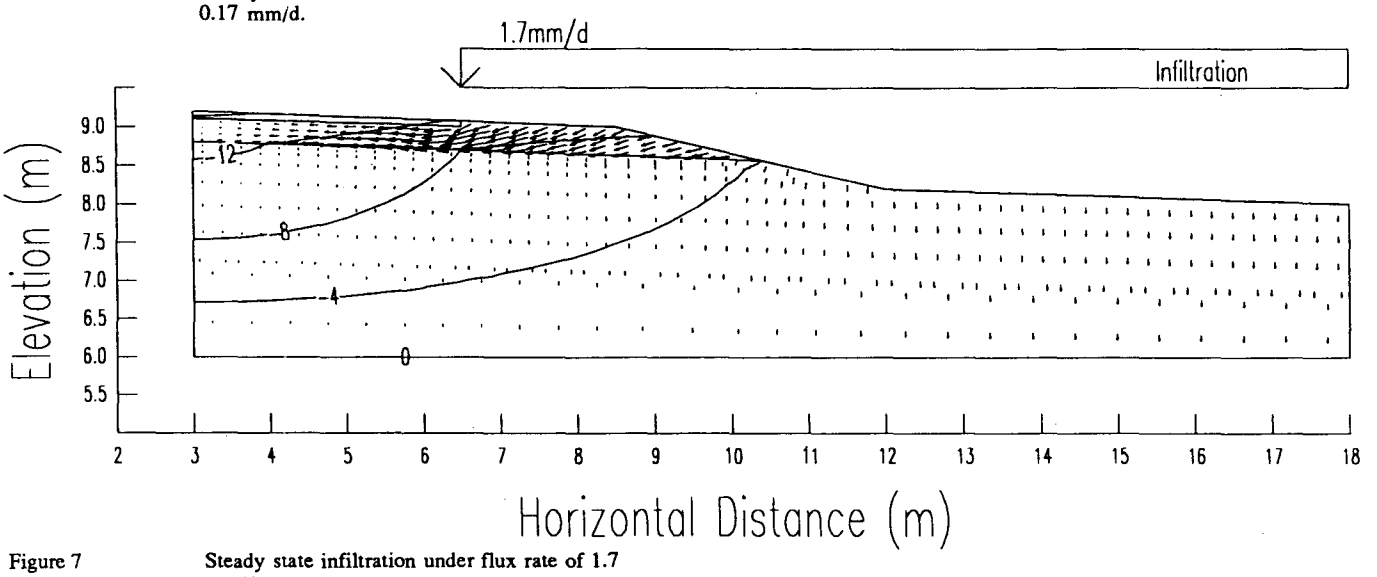

Figure 7 Steady state infiltration under flux rate of 1.7 mm/d.

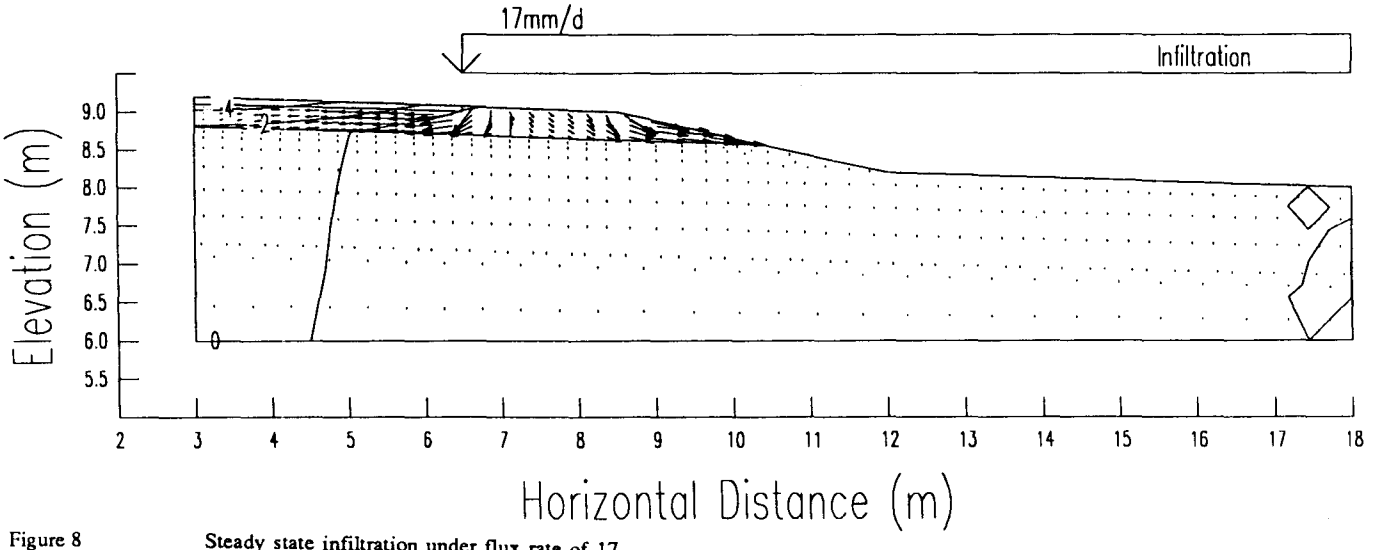

Figure 8 Steady state infiltration under flux rate of 17 mm/d.

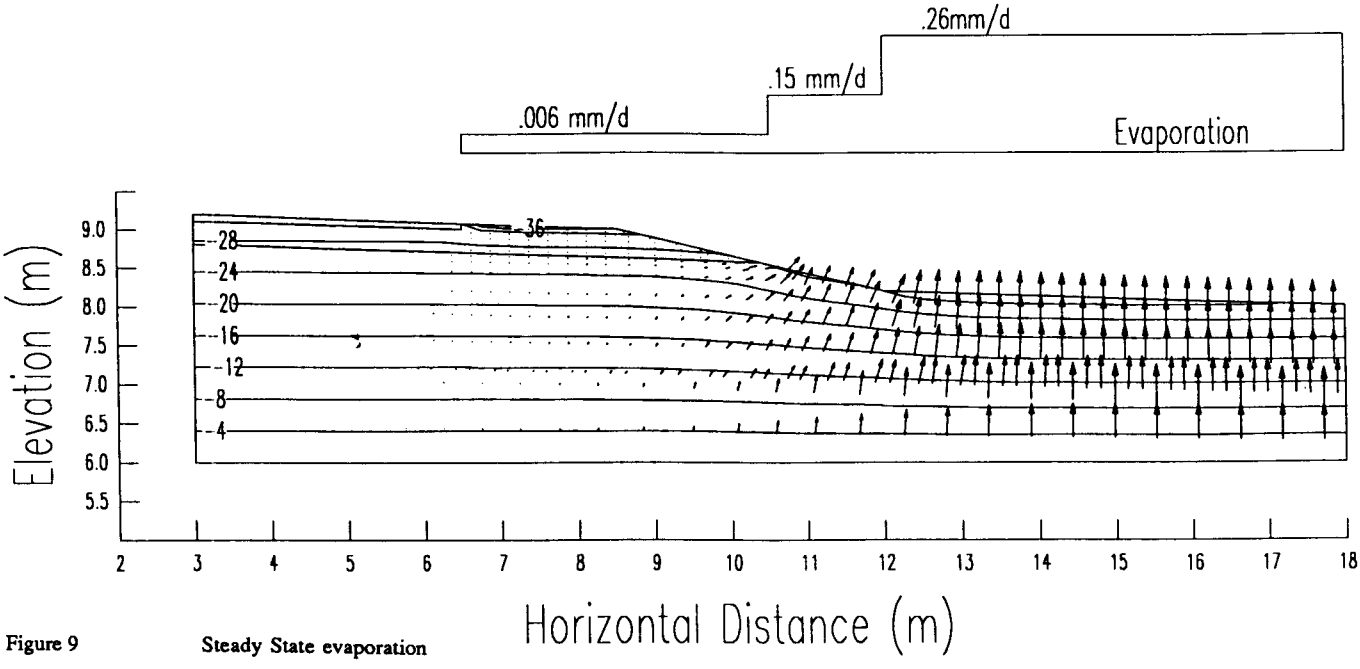

Figure 9 Steady State evaporation

the integrated circuit type thermal conductivity sensor, the temperature rise is converted into a voltage reading. Due to the higher thermal conductivity of water in comparison to air, a saturated tip at zero matric suction will register the lowest temperature rise due to the high heat loss by the water. The temperature rise is a function of the degree of saturation of the ceramic tip and not of the pressure of the water. The sensor, therefore, cannot measure positive pressures. Reasons for negative matric suction readings are discussed by Loi, Fredlund, Gan and Widger (1992).

In the second case history, eighteen thermal conductivity sensors were installed along a section of railway embankment in the Emerson Subdivision Trackage in the Winnipeg area, Manitoba, Canada. These sensors were installed in connection with the remedial design of some unstable sections of the embankment. Analysis concluded that berming would alleviate some of the instability problems.

Four sites were instrumented. At each instrumentation site, a trench was cut into the side of the embankment using a backhoe. The thermal conductivity sensors were installed at an upward angle into the side of the trench.

Typical data from the sensors at each of the four instrumentation locations are shown in Figures 21 to 24. No readings were collected during the period of December to April when the sensors were frozen. The higher thermal conductivity of ice and the unknown proportions of frozen and unfrozen water makes the sensor readings difficult to interpret. Also, the latent heat of fusion associated with the transformation of water has a significant influence on the thermal conductivity of the sensor during freezing and thawing (Fredlund, Gan and Rahardjo, 1991).

Matric suction data obtained from thermal conductivity Sensor No. 3 (Figure 21) indicated that matric suction decreased with a decrease in seasonal temperature. From September, 1989 to December, 1989, the matric suction readings obtained from Sensor No. 3 dropped from about 120 kPa to about 25 kPa. Readings taken over the next year also indicated that the matric suction reading decreased from a relatively high value in September to a lower value in November.

During the spring period, Sensor No. 3 registered a low matric suction of about 25 kPa. The matric suction reading began to increase after June 20, 1990, which corresponds to the beginning of out hot Prairie summer. This indicated a drying out of the embankment with time over the hot season. The matric suction readings reach a high of about 150 kPa in late August. From late August onwards to November, the matric suction readings decreased, probably due to the lower evaporation rate over the precipitation rate in the fall season.

Data from Sensor No. 6 as presented in Figure 22 did not show as much variation in matric suction with seasonal temperature as did Sensor No. 3. It did show, however, that the matric suctions recorded from May 1990 to October 1990 were consistently higher than the matric suctions recorded just after the sensor was installed. This would appear to indicate that the gravel layer within the berm was effective as a drain.

The data presented in Figure 23 for Sensor No. 8 would indicate that the gravel layer within the berm was not functioning as effectively as a drain. The lower matric suction readings during the second year indicated that the embankment is becoming wetter with time.

The data recorded for a sensor installed in the control section which was not subjected to any remedial work, (i.e., not bermed) are presented in Figure 24. The trend in the measured matric suctions show that the average long term suction was higher than the initial reading taken shortly after installation. This was probably due to some drying of the embankment. The average matric suctions recorded were generally much lower than those for the sensors within the berm sections. This suggests that the gravel layer within the berm did, in general, improve the drainage of the embankment.

CONCLUSIONS

Field evidence and numerical modelling studies show that the subgrade beneath a highway pavement eventually attains an equilibrium moisture condition. This equilibrium condition is largely controlled by the microclimate and the material used in the shoulder of the highway.

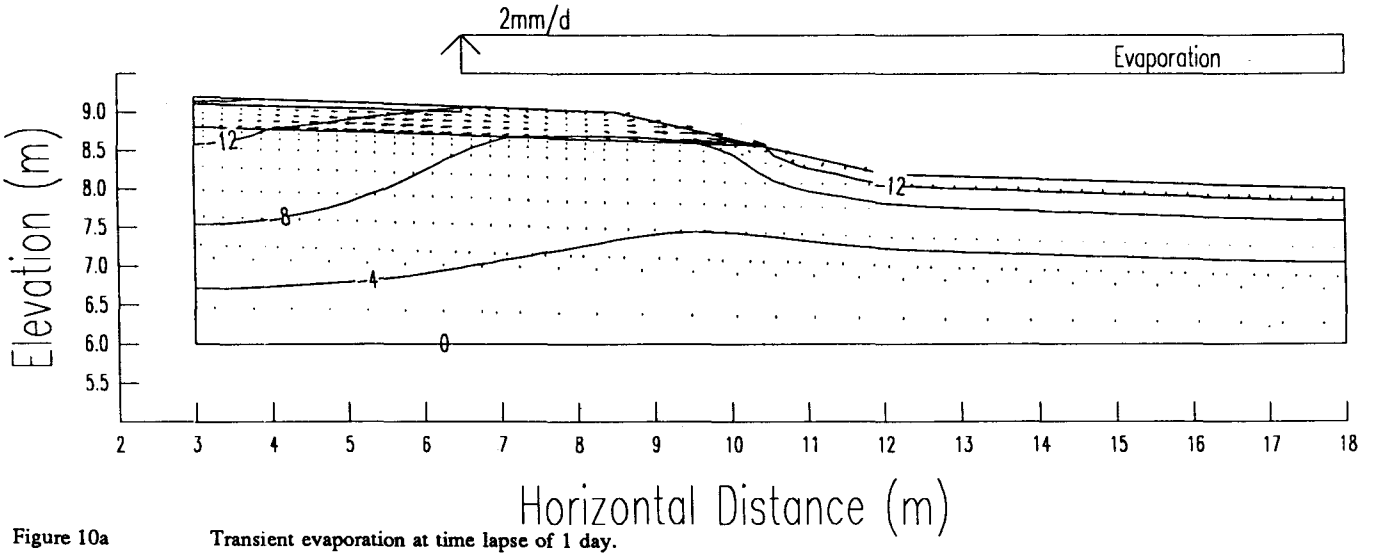

Figure 10a Transient evaporation at time lapse of 1 day.

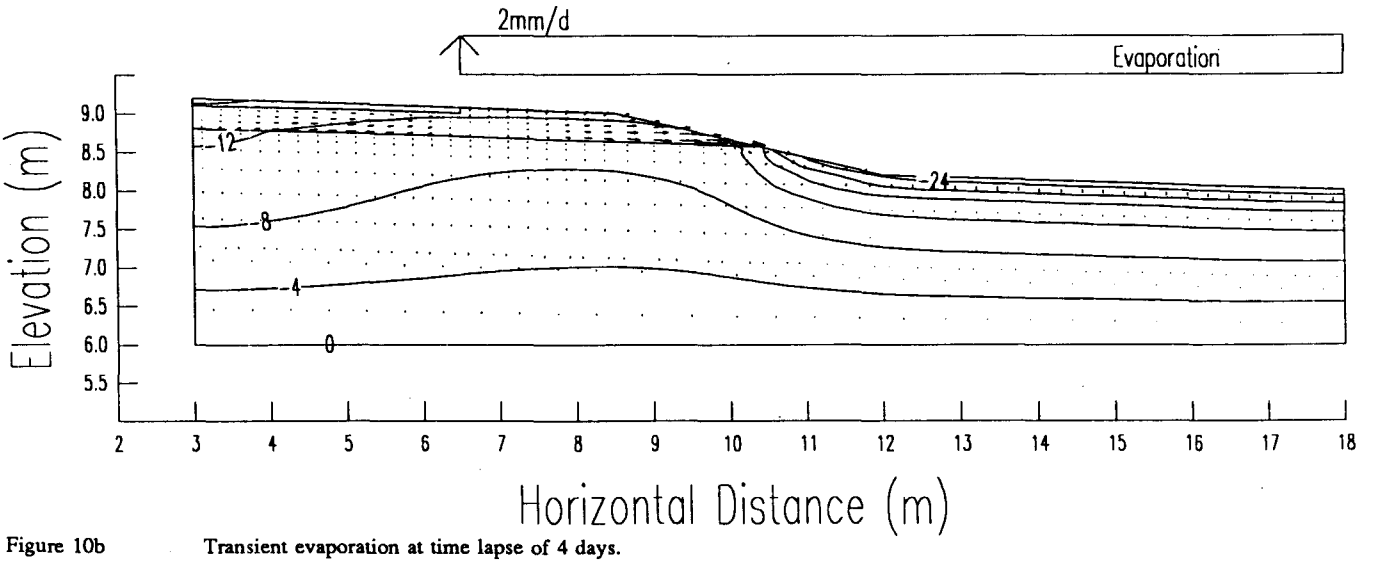

Figure 10b Transient evaporation at time lapse of 4 days.

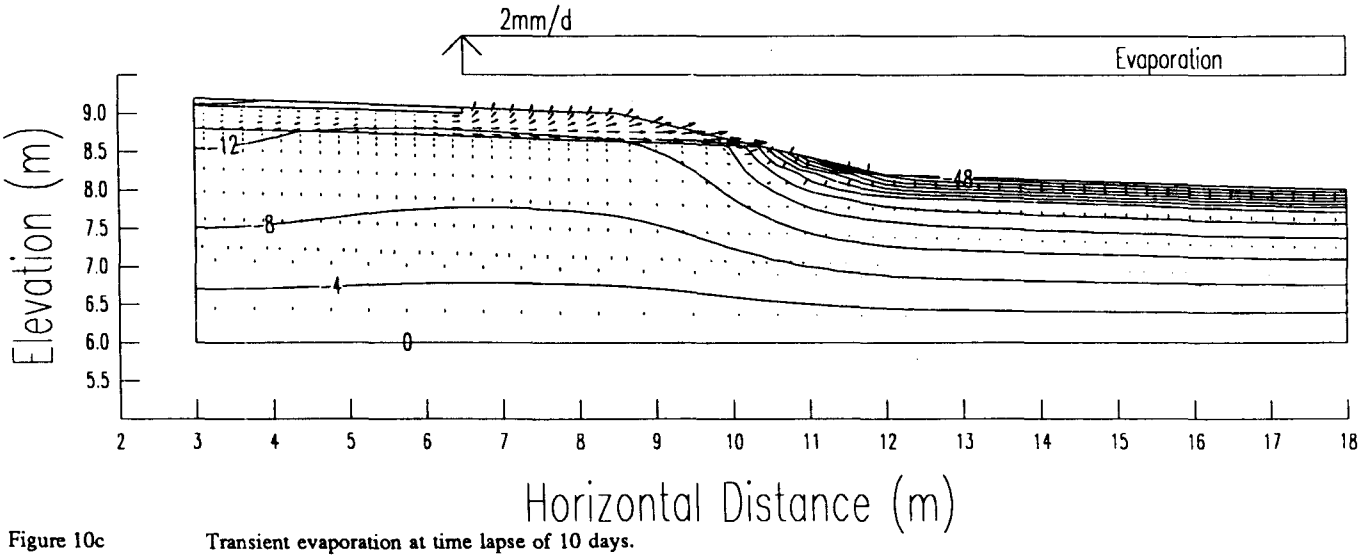

Figure 10c Transient evaporation at time lapse of 10 days.

The microclimate determines the flux boundary conditions. Infiltration tends to result in a wetting up of the subgrade beneath the pavement. This is due to strong lateral flows, especially under high flux rate. Evaporation, on the other hand, tends to induce a strong flow up across the shoulder and the ditch with little flow occurring near the center of the pavement.

Granular material, such as sand, has an actual evaporation rate which rapidly reduces to a rate of about 5 to 10 percent of the potential rate of evaporation after a short drying period. A clayey material, on the other hand, can maintain a high actual rate of evaporation over a long drying period. High infiltration and low evaporation rates will occur across the surface of a granular shoulder, resulting in a wetter subgrade. Increasing the clay or silt content of the shoulder would result in a drier and stronger subgrade beneath the pavement.

Thermal conductivity matric suction sensors appears to be a viable and practical method for field matric suction measurements.

REFERENCES

Aitchison, G. D., and B. G. Richards, "A Broad-Scale Study of Moisture Conditions in Pavement Subgrades Throughout Australia, Moisture Equilibria and Moisture Changes in Soils Beneath Covered Areas, A Symposium in Print", G. D. Aitchison, (Editor), Butterworths, Australia, pp. 184-232.

Barbour, S. L., 1990 "Reduction of Acid Generation in Mine Tailings Through the Use of Moisture-Retaining Cover Layers as Oxygen Barriers: Discussion." Canadian Geotechnical Journal, Vol. 27, No. 3, pp. 398-401.

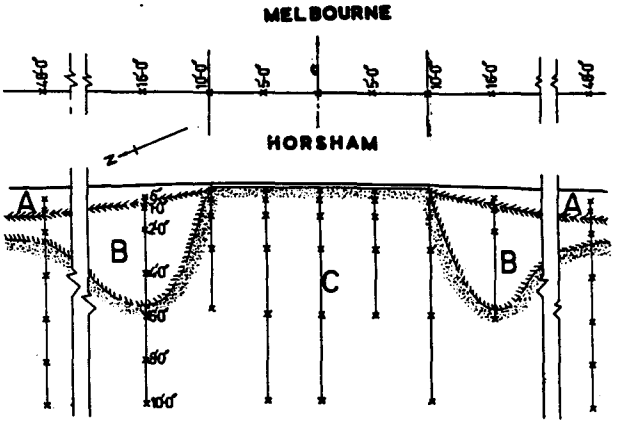

X = Location of probes.
A = Maximum seasonal variation in suction.
B = Significant change in suction (less than maximum).
C = No significant suction change.

Figure 11 Typical suction distribution below a highway structure in Horsham, Australia (from Aitchison and Richards, 1965).

Broms, B. B., 1965. "Effect of Degree of Saturation on Bearing Capacity of Flexible Pavements", Presented at the 43rd Annual Meeting of the Committee on Flexible Pavement Design, Ithaca, New York.

Brooks, R. H., and A. T. Corey, 1964. "Hydraulic Properties of Porous Media", Colorado State University Hydrol. Paper, No. 3, March.

Childs, E. C., and N. Collis-George, 1950. "The Permeability of Porous Materials", Proc. Royal Soc.., Vol. 201A, pp. 392-405.

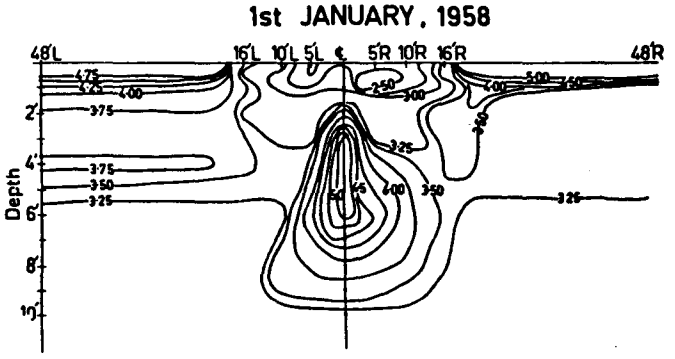

Gypsum block measurements of *pF*

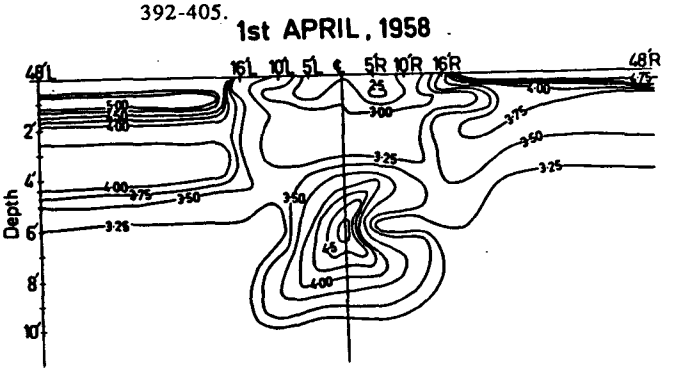

Gypsum block measurements of *pF*

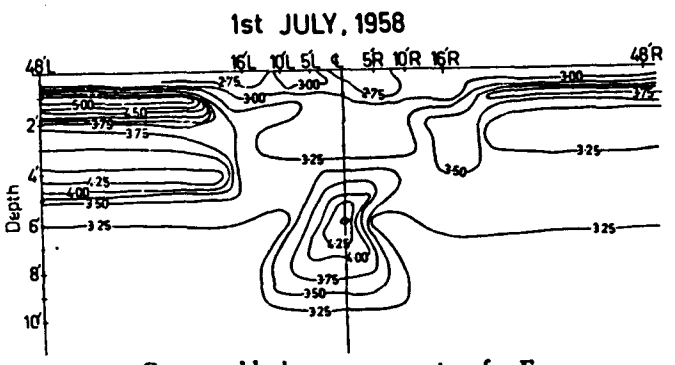

Gypsum block measurements of *pF*

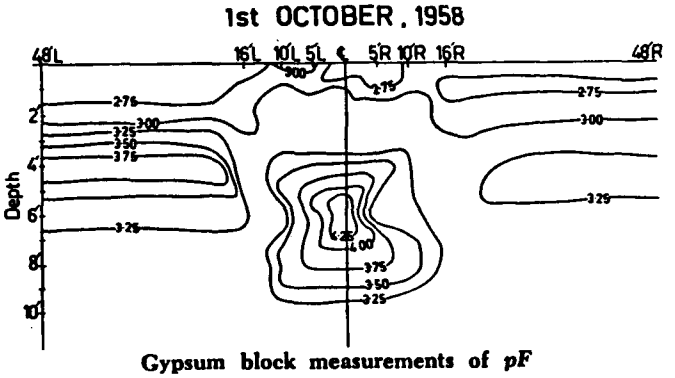

Gypsum block measurements of *pF*

Figure 12 Seasonal suction distribution below a highway structure in Horsham, Australia (from Richards, 1965).

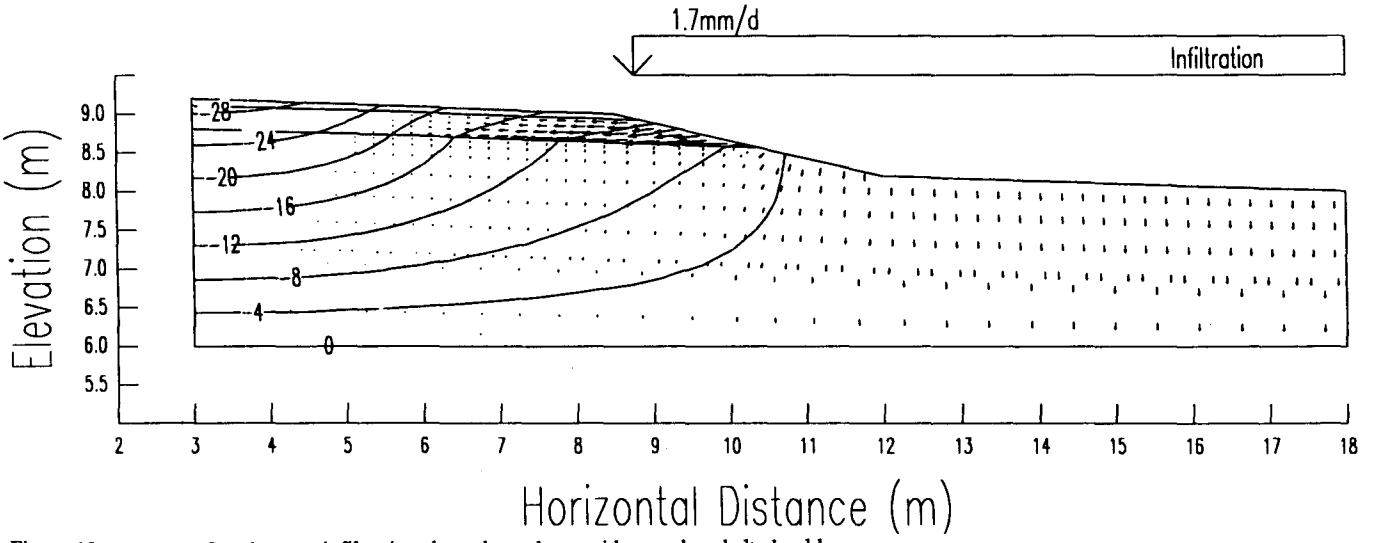

Figure 13 Steady state infiltration through roadway with paved asphalt shoulder.

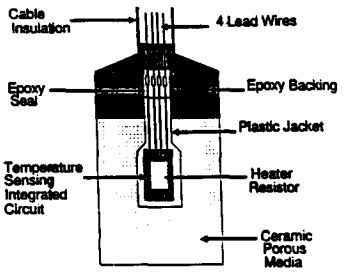

Figure 14 Schematic diagram of an integrated circuit type thermal conductivity matric suction sensor.

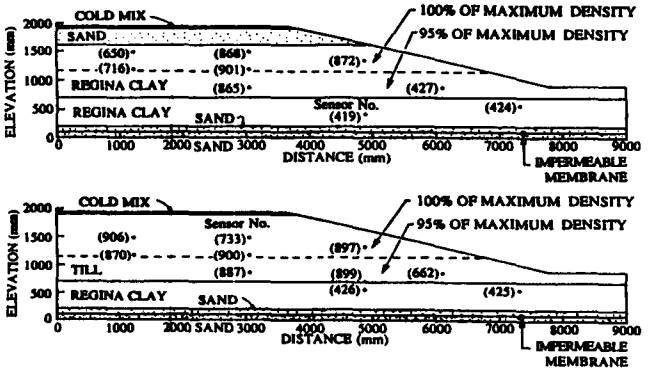

Figure 15 Cross sections of test track at Section 1A and Section 1B showing locations of sensors.

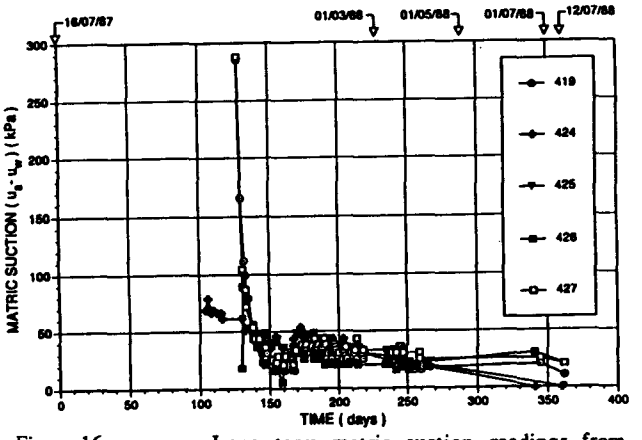

Figure 16 Long term matric suction readings from thermal conductivity matric suction sensor installed in pre-wetted holes.

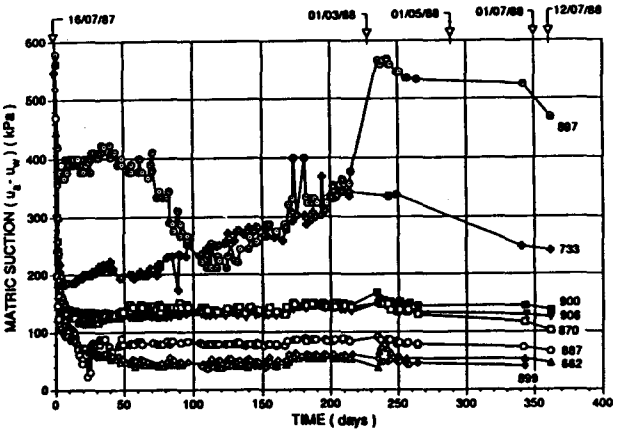

Figure 17 Long term matric suction readings in the till subgrade of test track.

Fredlund, D. G., and N. R. Morgenstern, 1976. "Constitutive Relations for Volume Change in Unsaturated Soils", Canadian Geotechnical Journal, Vol. 13, No. 3, pp. 261-276.

Fredlund, D.G., J. K. Gan, and H. Rahardjo, 1991. Measuring Negative Pore Water Pressures in a Freezing Environment. Transportation Research Record No. 1307, Transportation Research Board, National Research Council, pp. 291-299.

Gardner, W. R., 1958. "Laboratory Studies of Evaporation From Soil Columns in the Presence of a Water-Table", Soil Sci., Vol. 85, pp. 244-249.

GEO-SLOPE Int. Ltd., 1991. "SEEP/W - User's Guide", GEO-SLOPE Int. Ltd., Calgary, Alberta, Canada.

Gray, D. M., 1970. "Handbook on the Principles of Hydrology", Canadian National Committee for the International Hydrological Decade. National Research Council of Canada.

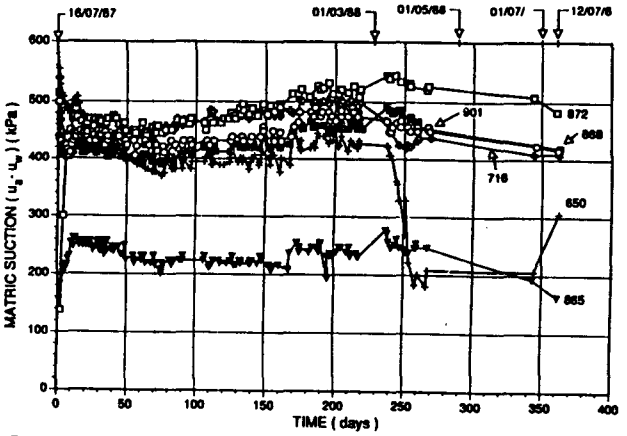

Figure 18 Long term matric suction readings in the clay subgrade of test track.

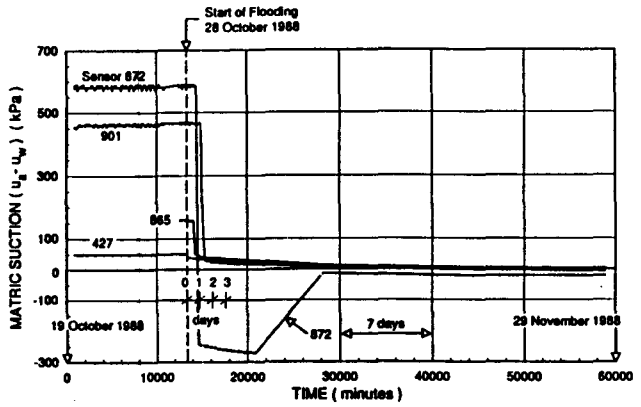

Figure 19 Responses of sensors located in the clay subgrade of test track.

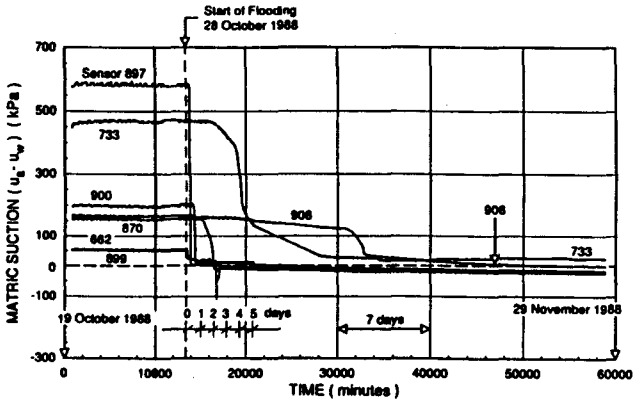

Figure 20 Responses of sensors located in the till subgrade of test track.

Green, A. E., and J. C. Corey, 1971. "Calculation of Hydraulic Conductivity: A Further Evaluation of Some Predictive Methods", Proc. Soil Sci. Soc. of Am., Vol. 35, pp. 3-8.

Holmes, R. M., 1961. "Estimation of Soil Moisture Content Using Evaporation Data", Proc. of Hydrology Symposium, No. 2 Evaporation, Queen's Printer, Ottawa, pp. 184-196.

Kisch, M., 1959. "The Theory of Seepage from Clay-Blanketed Reservoirs", Geotechnique, Vol. 9, pp. 9-21.

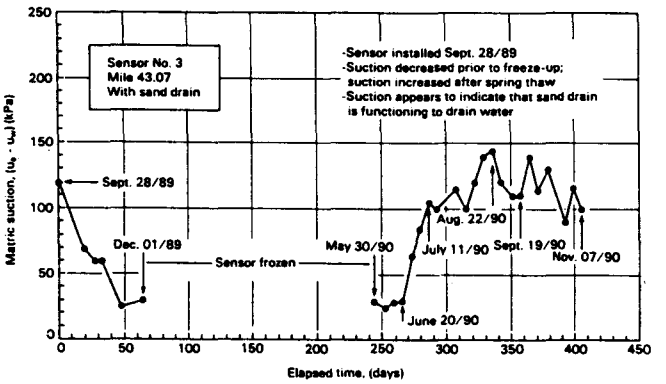

Figure 21 Matric suction readings from Sensor No. 3

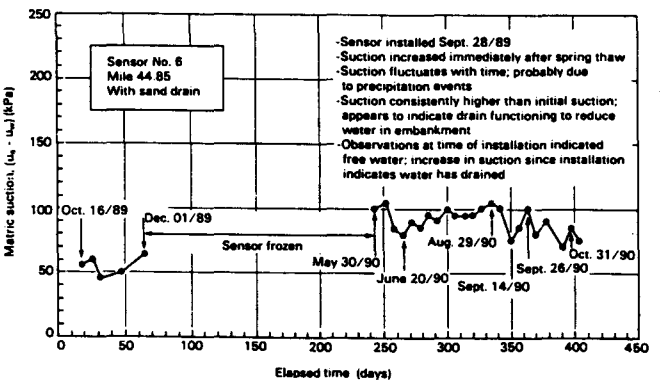

Figure 22 Matric suction readings from Sensor No. 6

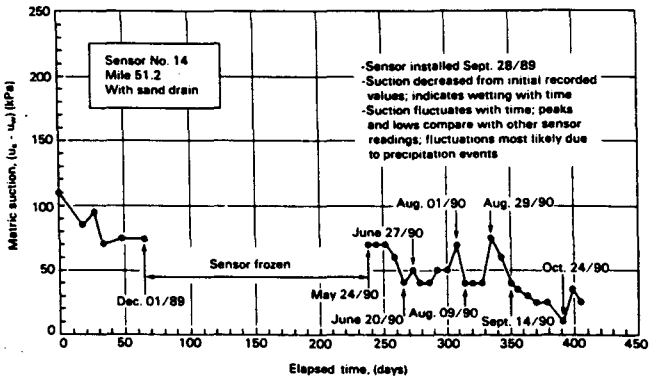

Figure 23 Matric suction readings from Sensor No. 14

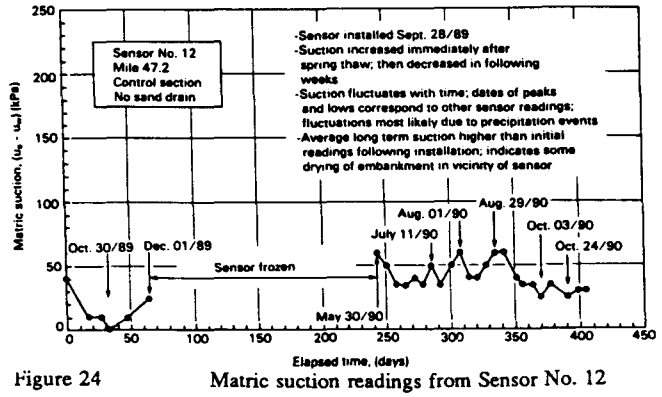

Figure 24 Matric suction readings from Sensor No. 12

Lam, L., D. G. Fredlund, and S. L. Barbour, 1987. "Transient Seepage Model for Saturated-Unsaturated Soil Systems: A Geotechnical Engineering Approach", Canadian Geotechnical Journal, Vol. 24, No. 4, pp. 565-580.

Loi, J., D. G. Fredlund, J. K. Gan, and R. A. Widger, 1992. "Monitoring Soil Suction in an Indoor Test Track Facility", Presented to the Transportation Research Board, 71st Annual Meeting, January 12-16, Washington, D. C.

Millington, R. J., and J. R. Quirk, 1961. "Permeability of Porous Solids", Trans. of the Faraday Soc., Vol. 57, pp. 1200-1207.

Maulem, Y., 1986. Hydraulic Conductivity of Unsaturated Soils: Prediction and Formulas. Methods of Soil Analysis, Part 1. Physical and Mineralogical Methods -- Agronomy Monograph No. 9 (2nd Edition). American Society of Agronomy. pp. 799-823.

Papagianakis, A. T., and D. G. Fredlund, 1984. "A Steady State Model for Flow in Saturated-Unsaturated Soil", Canadian Geotechnical Journal, Vol. 21, No. 3, pp. 419-430.

Richards, B. G., "An Analysis of Subgrade Conditions at the Horsham Experimental Road Site Using the Two-Dimensional Diffusion Equation on a High-Speed Digital Computer", Moisture Equilibria and Moisture Changes in Soils Beneath Covered Areas, A Symposium in Print, G. D. Aitchison, Editor, Butterworths, Australia, pp. 243-258.

Tschebotarioff, G. P., 1951. "Soil Mechanics, Foundations, and Earth Structures: An Introduction to the Theory and Practice of Design and Construction", McGraw-Hill, New York.

Van Genuchten, M. T.., 1980. "A Closed-Form Equation for Predicting the Hydraulic Conductivity of Unsaturated Soils", Journal of the Soil Science Soc. of Am., Vol. 44, pp. 892-898.

Wilson, G. W., 1990. "Soil Evaporative Fluxes for Geotechnical Engineering Problems", Ph.D. Dissertation, University of Saskatchewan, Saskatoon, Canada.